
PredDiff: Explanations and Interactions from Conditional Expectations

Stefan Blücher¹ Nils Strodthoff²

Abstract

PredDiff is a model-agnostic, local attribution method that is firmly rooted in probability theory. Its simple intuition is to measure prediction changes when marginalizing out feature variables. In this work, we clarify properties of *PredDiff* and put forward several extensions of the original formalism. Most notably, we introduce a new measure for interaction effects. Interactions are an inevitable step towards a comprehensive understanding of black-box models. Importantly, our framework readily allows to investigate interactions between arbitrary feature subsets and scales linearly with their number. We demonstrate the soundness of *PredDiff* relevances and interactions both in the classification and regression setting. To this end, we use different analytic, synthetic and real-world datasets.

1. Introduction

Understanding complex machine learning models is fundamental for high-stake applications in e.g. health care or criminal justice. To this end the Explainable AI (XAI) community has put forward a plethora of different attribution methods. One popular approach are post-hoc attribution methods, which can be broadly categorized according to the following properties: (i) local vs. global and (ii) model-specific (Bach et al., 2015; Lundberg et al., 2020) vs. model-agnostic (Ribeiro et al., 2016; Lundberg & Lee, 2017; Sundararajan et al., 2017). Here, we focus on the category of local, model-agnostic methods as the most versatile class.

In this work, we revisit Prediction Difference analysis (*PredDiff*), which was originally introduced in (Robnik-Sikonja & Kononenko, 2008). In our opinion, the beauty of *PredDiff* lies in its simplicity and strong connection to probability theory. The whole formalism is fixed by marginalizing out variables and measuring prediction differences. Since everything is defined on an instance-wise level, each instance’s prediction serves as its own reference point. This is why the formalism remains free of any potentially ambiguously

defined external reference points. On a conceptual level, the formalism approach leaves very little room for ambiguities. This advocates *PredDiff* as a baseline method for perturbation-based attribution methods and highlights the importance of understanding its capabilities and limitations. On a practical level, *PredDiff* has already been successfully applied in image classification settings (Zintgraf et al., 2017; Tian & Cai, 2017; Wei et al., 2018; Gu & Tresp, 2020).

However, there is a lack of theoretical and experimental understanding of *PredDiff*—a gap in the research landscape we want to fill with this work. In general, *PredDiff* relevances can be evaluated for arbitrary subsets of features and inherently incorporate interaction effects. Going one step further, one can even quantify them by means of a novel relevance measure for interaction effects between two arbitrary feature subsets. Importantly, this measure keeps the original linear scaling with the number of features. We introduce a concise unified notation for classification and regression tasks and show how quantified interaction effects can resolve apparent paradoxes in feature relevances and can lead to deeper insights into the model behavior. Interestingly, the consideration of the interaction relevance singles out logarithmic differences as the proper way to measure relevances, whereas all other commonly used difference measures fail to yield a vanishing interaction relevance for non-interacting features. In order to strengthen the probabilistic interpretation, we argue in favor for calibrating models as part of the interpretation scheme. This results in improves the clarity of attributions and avoids saturation issues observed in previous studies.

We demonstrate, based on synthetic and real-world datasets, how the combination of relevances and interactions leads to an improved model understanding. In summary, our main contributions are

- clarification of the theoretical foundations of *PredDiff*,
- definition of a novel, scalable feature interaction measure for model-agnostic model explanations,
- experimental verification on synthetic and real-world tabular datasets.

Both authors contributed equally. ¹TU Berlin, Berlin, Germany
²Fraunhofer Heinrich Hertz Institute, Berlin, Germany. Correspondence to: Nils Strodthoff <nils.strodthoff@hhi.fraunhofer.de>.

Code to reproduce our results can be found in our [GitHub](#) repository.

2. PredDiff: a local, model-agnostic, probabilistically sound attribution method

2.1. Relevances for classification and regression tasks

We consider a classification task, where a classifier f_c provides access to the conditional probability of class c given (sets of) input features x_i and y_i i.e. $f_c(x_i, y_i) := p(c|x_i, y_i)$. Here, (x_i, y_i) denotes the input features of the i th example. One way of assessing the relevance of a particular set of features y , is to compare the original prediction $p(c|x_i, y_i)$ to the prediction $p(c|x_i)$, where y has been removed. For an arbitrary classifier this can be implemented in a probabilistically sound manner by m -arginalizing out y (Robnik-Sikonja & Kononenko, 2008), i.e. via

$$m_{y|x_i}^{f_c} := p(c|x_i) = \int p(c|x_i, y)p(y|x_i)dy \quad (1)$$

$$= \int f_c(x_i, y)p(y|x_i)dy.$$

The integral can be evaluated by sampling from an appropriate generative model that samples from $p(y|x_i)$, see Appendix A for details. forwardly obtains confidence intervals for relevance scores via empirical bootstrapping. In this sense the approach is completely domain- and task-agnostic, provided an appropriate generative model for imputation is available. The ability to transparently exchange the imputer is a central advantage of this approach and encompasses different existing approaches, see the discussion below. Unlike for Shapley values (Janzing et al., 2020), it is clear that the conditional should be used in Equation (1). Additionally, ignoring feature dependencies unavoidably leads to simple adversarial attack strategies, see (Slack et al., 2020; Anders et al., 2020). Conditional sampling avoids evaluating the classifier far from the data manifold, which is an issue for many other perturbation-based attribution methods.

Note also that in Equation (1), class-wise probabilities rather than logarithmic probabilities are to be used. The latter are commonly used in many popular attribution frameworks. The connection to probability theory of our approach, however, clearly favors class-wise probabilities.

One then considers centered values by comparing to the predicted value at the datapoint. Several possibilities have been proposed in the literature (Robnik-Sikonja & Kononenko, 2008). Here, we compare logarithmic differences, which come with an interpretation of the information difference conveyed by y , i.e.

$$\bar{m}_{y|x_i}^{f_c} := \log_2 f_c(x_i, y_i) - \log_2 m_{y|x_i}^{f_c}, \quad (2)$$

see Section 2.2 for a justification of this choice. Here, we avoid issues with vanishing probabilities as in (Robnik-Sikonja & Kononenko, 2008) by means of a Laplace correction i.e. by mapping $p \rightarrow (pN + 1)/(N + K)$, where N is the number of training instances and K the number of classes. As second remark, we stress that Equation (1) is only valid, if the classifier output f_c can be identified with a proper probability distribution, i.e. for a *well-calibrated classifier*. In this work, we use temperature-scaling to achieve this (Guo et al., 2017).

Turning to regression problems, where we try to infer relevances with respect to a particular function $f(x_i, y_i)$. Hence, only the class subscript in Equation (1) is suppressed. For a regression task, the target is directly meaningful and therefore, we directly consider centered m -values via

$$\bar{m}_{y|x_i}^f := f(x_i, y_i) - m_{y|x_i}^f, \quad (3)$$

with a slight abuse of notation. Our notation aims to unify regression and classification tasks as far as possible.

It is worthwhile stressing that x and y are to be understood as partitions of the full set of features, and therefore, refer to sets of features rather than individual features. The formalism allows to obtain relevances for arbitrary combinations of features.

Upon varying the imputation function, *PredDiff* encompasses a number of existing approaches. Most notably this includes occlusion based approaches, where $p(y|x_i)$ returns the mean or the median value of y and generative model approaches that approximate the integral by a single sample (Lenis et al., 2020). Various degrees of sophistication are conceivable ranging from random sampling from the training set (Robnik-Sikonja & Kononenko, 2008) to multivariate Gaussian imputers (Zintgraf et al., 2017) onto sampling uniform super-pixels (Wei et al., 2018). The latter is a good example for the inherent connection between model and the data distribution it was trained on. This connection can be leveraged to improve imputers and provides a clear path towards improved attribution scores. We implemented a range of imputers for tabular data in the accompanying code repository that are described in Appendix B. Lastly, it is worth noting that all model-agnostic interpretation methods depend on input perturbation and, consequently, need to specify an imputation algorithm.

We discuss different properties of *PredDiff* attributions in Appendix C. In particular, we show the *dummy player* property, i.e. yield a vanishing relevance $\bar{m}_{y|x_i}^{f_c} = 0$, if the function under consideration does not depend on y . It is important to note, that *PredDiff* is not an additive attribution method, where the sum of all feature relevances adds up to the predicted output. As remarked by (Gosiewska & Biecek,

2020), this should be seen as an asset rather than a liability in the light of feature interactions within complex non-additive models. Due to this fact, it completely avoids the necessity to implicitly or explicitly define a reference sample that conveys a complete absence of signal. Every sample and feature can in a sense be seen as its own reference value.

2.2. Interaction relevances

Until here we have introduced well-defined relevances for distinct sets of variables, see Equation (2) and Equation (3). We now want to go a step further and quantify how much relevance can be attributed to the interaction between two feature sets.

Here, we consider two interacting non-overlapping feature sets y and z and denote the remaining features by x . We start our discussion in the context of regression as it is slightly more intuitive. The idea is to decompose the joint relevance $\bar{m}_{y,z|x_i}^f$ into two independent terms related to the individual relevances and treat the remainder as interaction. This idea is based on the assumption to obtain a vanishing interaction relevance in case of a purely additive function, e.g.

$$f(x, y, z) = f_y(x, y) + f_z(x, z). \quad (4)$$

We refer to this property as *no-interaction* property. In this case, the joint relevance from Equation (3) decomposes into

$$\bar{m}_{y,z|x_i}^f = \bar{m}_{y|x_i}^{f_y} + \bar{m}_{z|x_i}^{f_z}. \quad (5)$$

As we require the interaction relevance to vanish in this case, considering the difference between both sides of the above equation is a natural candidate for an interaction measure.

It remains to generalize $\bar{m}_{y|x_i}^{f_y}$ to general f . There are two obvious generalizations to deal with the potential z -dependence that preserve the property from above. Firstly, by evaluating at $z = z_i$, i.e. $\bar{m}_{y|x_i}^{f|z=z_i}$, or secondly, by marginalizing, i.e. $\bar{m}_{y|x_i}^{\int f(x_i, y, z)p(z|x_i, y)dz}$. Here, we work with the former definition as it relates more closely to the relevance definition in Equation (1). Therefore, we define the *interaction relevance* via

$$\bar{m}_{y;z|x_i}^{\text{int},f} := \bar{m}_{y|x_i}^{f|z=z_i} + \bar{m}_{z|x_i}^{f|y=y_i} - \bar{m}_{y,z|x_i}^f, \quad (6)$$

which by construction vanishes for a function f of the form Equation (4). All expressions involved can be approximated by sampling from $p(y, z|x_i)$, see Appendix A for details. Note that our motivation for Equation (6) does not fix the sign of the interaction relevance. One can easily convince oneself for simple examples, such as those in Section 4.1, that the sign choice from above is a reasonable choice.

In analogy to (Lundberg et al., 2020; Fujimoto et al., 2006),

we define *residual feature relevances* by removing interaction contributions

$$\bar{m}_{y|y_i^c}^{\text{res},f} := \bar{m}_{y|y_i^c}^f - \sum_{z \neq y} \bar{m}_{y;z|(y \cup z)_i^c}^{\text{int},f}, \quad (7)$$

where y^c denotes the complement of feature set y with respect to the set of all features. Here, the sum includes all non-overlapping feature sets not including the target features y .

In the classification setting, we consider a generalization of *informative conditional interactions* (Jakulin & Bratko, 2003), implying that there is no label c and residual features x such that the feature sets y and z directly interact, as a constraint for a non-interacting classifier i.e.

$$p(y, z, x|c) = p(x, y|c)p(x, z|c). \quad (8)$$

If we additionally impose conditional independence of y and z given x alone as a constraint on the data distribution, we can show that the interaction relevance from Equation (6) between y and z indeed vanishes under the given conditions, see Appendix D for a derivation, satisfying the *no-interaction* property. This means that Equation (6) upon replacing f by f_c can be equally applied in the classification setting. Here, it is worth stressing that the *no-interaction* property singles out logarithmic differences in Equation (2) and does not hold for other popular difference measures such as raw probabilities or log-odds (Robnik-Sikonja & Kononenko, 2008).

3. Related Work

PredDiff was originally introduced in (Robnik-Sikonja & Kononenko, 2008). Subsequently, *PredDiff* was reconsidered for image classification applications in the deep learning literature, see for example (Zintgraf et al., 2017; Tian & Cai, 2017; Wei et al., 2018; Gu & Tresp, 2020). Other notable contributions in this direction are (Lemaire et al., 2008; Datta et al., 2016; Casalicchio et al., 2019). However, all previous studies miss a comprehensive treatment in a well-controlled setting, testing analytical and experimental limits of *PredDiff*. From a broader perspective, *PredDiff* encompasses other attribution methods that rely on altering input samples and measuring the corresponding prediction changes. In computer vision, popular approaches in this respect are partially occluding images (Zeiler & Fergus, 2014) or inpainting image parts with generative models, see (Agarwal & Nguyen, 2020; Lenis et al., 2020). Such single-sample approximations of Equation (2) are, however, potentially unreliable, see Figure 2, and therefore not covered by the foundations of *PredDiff*.

Other popular local model-agnostic attribution methods include LIME (Ribeiro et al., 2016), Integrated Gradients (Sundararajan et al., 2017) and Shapley-value based approaches (Lundberg & Lee, 2017; Štrumbelj & Kononenko, 2010; 2013). All of them are based on perturbing individual instances, see (Covert et al., 2020) for a unifying perspective. However, they differ from the proposed approach in terms of how they treat changing prediction outcome. Importantly, also axiomatically well-defined frameworks leave ambiguities when used for practical model explanation. Prominent questions are whether to sample from conditional or marginal distributions, see e.g. (Janzing et al., 2020), or whether to base relevances for classification task on class-wise probabilities rather than their logarithms. This is in contrast to the *first principle* definition in Equation (1) that is solely based on probability theory.

The second main aspect of this work, the incorporation and quantification of feature interactions, has very recently attracted interest within the interpretability community. First works on interaction effects appeared (Tian & Cai, 2017; Janizek et al., 2020; Deng et al., 2020; Schnake et al., 2020). Additionally, interaction measures have been proposed for Shapley-value-based approaches (Gosiewska & Biecek, 2020; Lundberg et al., 2020; Sundararajan et al., 2020; Zhang et al., 2021), global ALE-plots (Apley & Zhu, 2020), and other perturbation-based approaches (Jin et al., 2020; Tsang et al., 2020). However, most approaches remain limited to binary interactions between individual features. *PredDiff* has the particular advantage that it allow to quantify interaction effects between two arbitrary (non-overlapping) features set, while remaining a linear scaling.

4. Experiments

Until now, we have promoted *PredDiff* as a simple and intuitive framework for local model interpretation. In the following sections, we will test its practical usefulness on different datasets and learning tasks, each supporting different advantages of *PredDiff*.

4.1. Analytic examples

We consider a generic function $f(x, y, z) = f_y(x, y) + f_z(x, z) + h(x, y, z)$ with an arbitrary associated data distribution $p(x, y, z)$. We can then easily deduce

$$\bar{m}_{y|x_i, z_i}^f = \bar{m}_{y|x_i, z_i}^{f_y} + \bar{m}_{y|x_i, z_i}^h, \tag{9}$$

$$\bar{m}_{y; z|x_i}^{\text{int}, f} = \bar{m}_{y; z|x_i}^{\text{int}, h}, \tag{10}$$

which are also just simple consequences of linearity and the dummy/no interaction properties. As an explicit example for the dummy property, note that Equation (9) no longer depends on the irrelevant f_z parts. Moreover, *PredDiff* in Equation (10) successfully recovers the original

Table 1. *PredDiff* (interaction) relevance for $f(x_a, x_b) = x_a \vee x_b$ and a uniform underlying data distribution (up to a constant $1/4$).

(x_a, x_b)	(0, 0)	(1, 0)	(0, 1)	(1, 1)
$\bar{m}_{x_a x_b}$	-2	+2	0	0
$\bar{m}_{x_b x_a}$	-2	0	+2	0
$\bar{m}_{x_a x_b}^{\text{res}}$	-1	+1	-1	+1
$\bar{m}_{x_b x_a}^{\text{res}}$	-1	-1	+1	+1
$\bar{m}_{x_a;x_b}^{\text{int}}$	-1	+1	+1	-1

interaction part h . We now further specify $h(x, y, z) = h_y(x, y) \cdot h_z(x, z)$ together with a factorizing probability distribution $p(y, z|x) = p(y|x)p(z|x)$. Using this multiplicative interaction we can derive

$$\bar{m}_{y; z|x_i}^{\text{int}, h} = \bar{m}_{y|x_i}^{h_y} \cdot \bar{m}_{z|x_i}^{h_z}. \tag{11}$$

Again we observe an intuitive behavior which recovers the original multiplicative form.

As second explicit example, we revisit a famous example from (Štrumbelj & Kononenko, 2010; 2013), that is often used as an argument against approaches along the line of *PredDiff*. We consider two binary input variables x_a and x_b that are sampled uniformly i.e. are subject to the data distribution $p(x_a, x_b) = \frac{1}{4}$. The function under consideration is $f(x_a, x_b) = x_a \vee x_b$. For consistency with the literature, we work in a regression setting, but the same qualitative conclusions can be drawn from a classification setting. The apparent paradox arises from the fact that the single feature relevances vanish if the other, conditioned variable is set to 1. Explicitly this means, that $\bar{m}_{x_a|x_b} = 0$ if $x_b = 1$ as the outcome of $x_a \vee x_b$ is already completely specified for $x_b = 1$. The same applies to $\bar{m}_{x_b|x_a}$ for $x_a = 1$, from which (Štrumbelj & Kononenko, 2010; 2013) incorrectly conclude that neither x_a nor x_b are relevant for the prediction in this case. This apparent contradiction is obviously resolved by incorporating interaction effects: Firstly, we note that all residual single feature interactions are positive (negative) for a value of one (zero). Secondly, the combined interaction relevance is only positive in the exclusive or combination. For reference, we also include a similar analysis of $x_a \vee x_b$ in a classification setting in Appendix E.

4.2. Regression: Synthetic datasets

This section aims to validate the definitions for both single feature contribution and feature interaction based on a synthetic regression task. The main message we try to convey is that *PredDiff* successfully grasps the relevant contributions for model-agnostic interpretation.

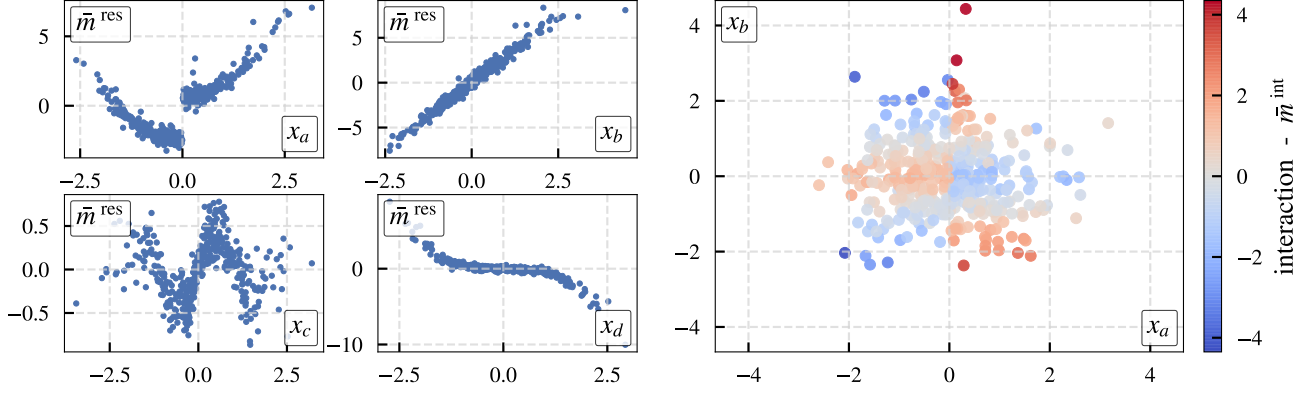


Figure 1. *PredDiff* contributions for synthetic regression task. LEFT: $\bar{m}^{\text{res},f}$ according to Equation (7). All additive terms are successfully captured. Feature x_a causes a monotonic positive (or negative) interaction contribution. Hence, an additional reminiscent, discontinue effect appears at $x_a = 0$. Compare to Figure 2 for raw feature contribution of x_b . RIGHT: color-encoded $\bar{m}^{\text{int},f}$ interaction relevance Equation (6) between feature x_a and x_b , which is analytically given by $\text{sgn}(x_a) |x_b|$. Based on $N = 200$ imputations generated with a multivariate Gaussian imputer and an underlying random forest regressor.

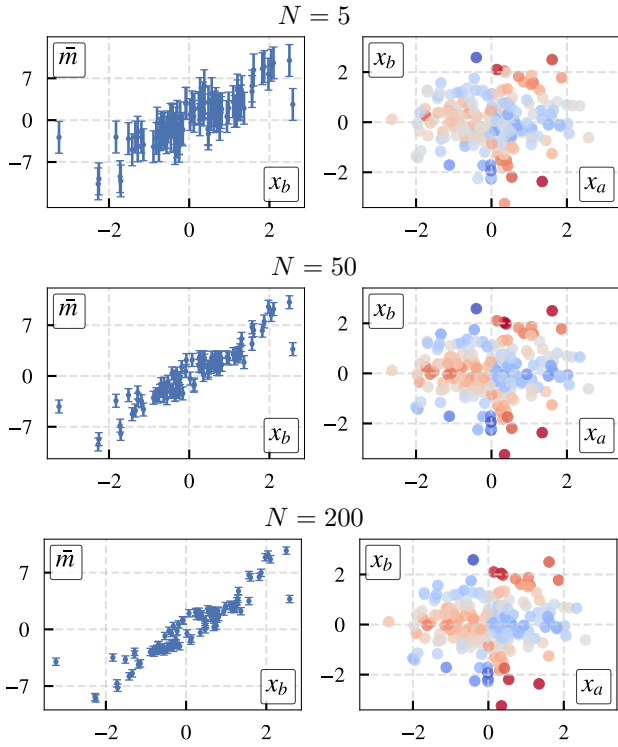


Figure 2. Visualizing computational dependence of *PredDiff*; N : number of imputations. LEFT: $\bar{m}_{x_b}^f$ according to Equation (3). High statistical accuracy needed to resolve branching caused by the interaction. RIGHT: color-encoded $\bar{m}^{\text{int},f}$ interaction relevance Equation (6) between feature x_a and x_b . The colorbar is approximately equal to Figure 1.

We consider a synthetic dataset with four different features x_a, \dots, x_d . These features are generated by a Gaussian distribution with mean 1 and independent covariances $\Sigma = \mathbb{1}_4$. Additionally, we defined an target function $f : \mathbb{R}^4 \rightarrow \mathbb{R}$:

$$f(x) = x_a^2 + 3x_b + \sin(\pi x_c) - \frac{x_d^3}{2} + 2 \text{sgn}(x_a) \text{abs}(x_b). \quad (12)$$

This target is composed out of four additive feature contribution. Additionally, we added an interaction term between feature a and b . At this point we want to stress that this choice is rather arbitrary. However, we believe that the results and conclusions are generic and invite the reader to try different functional forms in the accompanying notebook. In this section, we present results for a *Random Forest* regressor trained on 3600 samples. Since *PredDiff* is model-agnostic, however, we present results for other regression algorithms in Appendix F and compare our method to *TreeInterpreter* (Lundberg et al., 2020), which also provides an interaction measure.

In Figure 1, we show individual (residual) contribution, as in Equation (7), for all four individual features (left) and the interaction relevance (right) between feature a and b . Looking at the individual feature attribution first, we observe that all individual contribution are recovered correctly, e.g. the sinusoidal (x_c) or cubic (x_d) functional form are immediately recognizable. It is worth pointing out, that the individual contribution for feature c and d are not distorted by the additional corrections induced by the interaction formalism. In essence, this is the experimental manifestation of the *no-interaction* property previously stated. In summary, we can conclude that *PredDiff* reliably recovers additive contributions, which paves the way for successful treatment of

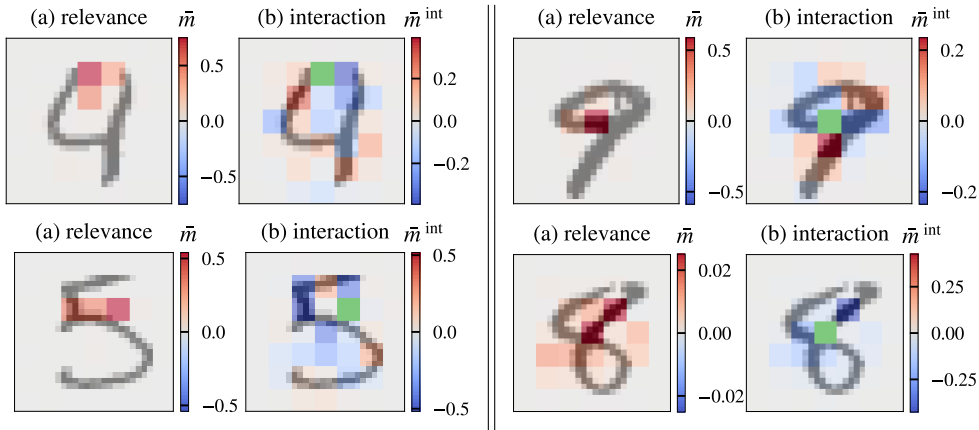


Figure 3. *PredDiff* for MNIST digits calculated on squared pixel batches ($\text{filter_size} = 4$) using a train set imputer. (a) relevance. (b) interaction with respect to the marked (green) reference super-pixel. We always selected the super-pixel with highest relevance. Further examples can be found in Appendix G.

interaction effects. We now turn to the interaction between features a and b . The color-encoded interaction relevance in Figure 1 clearly reveals the absolute value contribution of x_b combined with a sharp transition at $x_a = 0$ which is induced by the sign operation. The latter also explains the spurious jump at the origin in the residual contribution for x_a . Due to the sign operation, feature x_a has a monotonic positive or negative effect. Hence, a part of the interaction term can solely be contributed to feature x_a and causes the discontinuity at the origin. Please note, that this is in contrast to feature b , for which all interaction contributions are removed and only the linear dependence remains.

Next, in Figure 2 we demonstrate the scaling behavior of *PredDiff* relevances with the number of samples used to approximate Equation (1), a parameter which allows to adjust the computational demands of the approach significantly. This question also touches upon the reliability of different single-sample perturbation-based approaches used in the literature, which can be seen as single-sample approximations of *PredDiff*. On the left hand side the (non-residual) relevance \bar{m}^f of feature x_b is shown. This compares to the residual interaction $\bar{m}^{\text{res},f}$ in Figure 1. We observe that the interaction effects leads to two distinct branches. However, a large number of imputations N is needed to resolve this effect. In contrast, on the right hand side of Figure 2, the interaction effect is immediately obvious even for low statistical accuracy. This leads to the conclusion that our definitions have the correct functional form to extract suppressed high fidelity signals.

In contrast to other attribution methods *PredDiff* offers meaningful error bars without any additional overhead. This is particular important to balance the trade-off between statistical accuracy and computational costs.

As a final remark, this synthetic example was deliberately chosen rather simple in the sense of a very small number of input dimensions and no input correlations, which is not necessarily representative for the situation encountered by ML algorithms in the wild. This simplified scenario allows to train very accurate classifiers on the entire input domain. In particular, it does therefore not include potential issues arising from evaluating the model far from the data manifold, which is an issue many perturbation-based attribution methods have to face. A detailed study of the robustness properties *PredDiff* compared to existing approaches along the lines of (Slack et al., 2020; Anders et al., 2020) is an interesting direction for future research.

4.3. Classification: (Tabular) MNIST

In the previous section, we have established an intuitive global interpretation using local *PredDiff* attributions. In this section, we move forward and analyze the instance-wise attribution maps generated with *PredDiff*. To showcase the abilities of *PredDiff*, we use the MNIST dataset, which allows an intuitive interpretation of the resulting attribution maps and is not too small neither in terms of dataset size nor in terms of input dimensionality. As we focus on tabular datasets in this work, we flatten the images into 784-dimensional vectors and train a fully-connected classifier (hidden layers 1000 and 500) on the dataset. The model achieves an accuracy of 97.8% after $n_{\text{epochs}} = 10$ epochs of training. Additionally, the model is overconfident in its prediction, meaning that the predicted probability score are higher than the actual scores. To remedy this situation and enforce a proper probabilistic interpretation we calibrate the network using temperature scaling as proposed in (Guo et al., 2017). This is the natural way of dealing with potential saturation issues without the need to adjust the original formalism as in (Gu & Tresp, 2020).

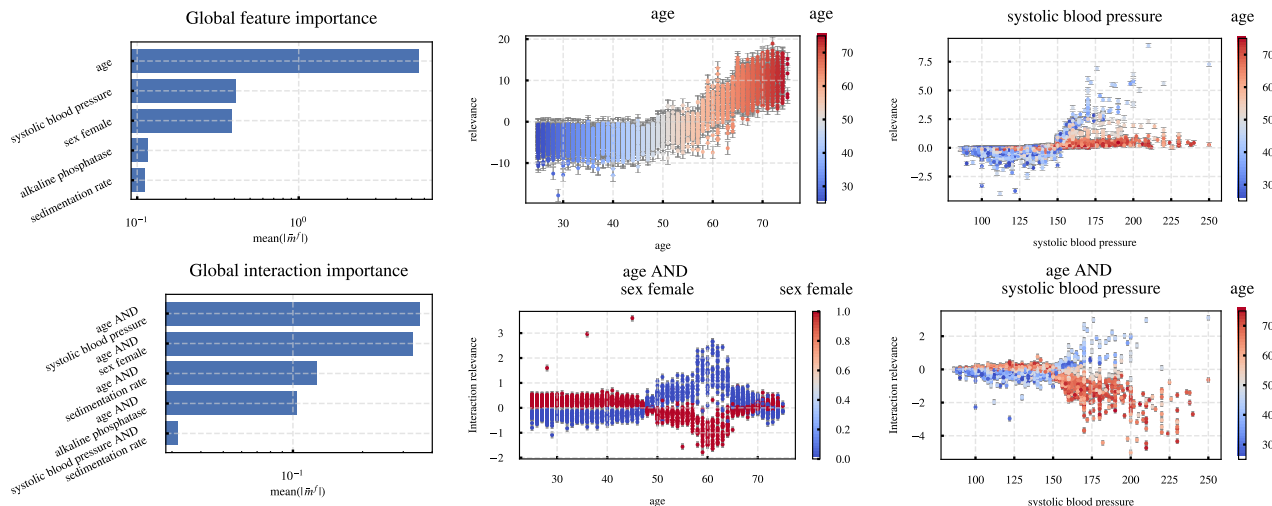


Figure 4. *PredDiff* (interaction) relevances for a *Random Forest* trained on the NHANES dataset using a Mahalanobis imputer (Aas et al., 2019) that are in qualitative agreement with existing methods (Lundberg et al., 2020). TOP LEFT: Ranking of the five most important features. TOP CENTER: Relevance for the most important feature age. TOP RIGHT: Relevance for the second most important feature systolic blood pressure. BOTTOM LEFT: Ranking of the five most important feature interactions. BOTTOM CENTER: Interaction relevance between systolic blood pressure and age. BOTTOM RIGHT: Interaction relevance between age and sex revealing a pronounced age dependence.

We analyze this calibrated model using *PredDiff* in the next step. Therefore, we define *super-pixels* using squared filters as our features of interest. However, *PredDiff* gives no restrictions on this selection, see (Wei et al., 2018; Tian & Cai, 2017) for an analysis using classical super-pixels. Importantly, this flexibility is retained by our novel interaction measure. Here, we use a train set imputer, as it offers realistic and versatile imputations for simple MNIST figures. Additionally, we show results for a variational autoencoder with pseudo-Gibbs sampling (Rezende et al., 2014), see Appendix B for details, in Appendix G. In Figure 3 (a) we show the corresponding attributions for four different digits. The digits are chosen to be a representative subset of the complete test set. We see that the attributions are visually reasonable, e.g. the characteristic white space for the four and five are highlighted or also the characteristic parts of figure eight and nine. This demonstrates *PredDiff*'s ability to also produce intuitively meaningful attributions.

In the next step, we analyze the interaction measure. To this end, we calculate the interaction between all super-pixels with respect to the super-pixel with highest relevance and show the resulting heatmap in in Figure 3 (b). The first thing to note is that the heatmaps are sparse and hence, informative. Our measure clearly highlights the intuitively related figure parts such as neighboring pixels. In contrast, if we would measure the combined effect of both pixels, the resulting heatmap would be blurry and covering up the main effects. The second interesting observation is the negative sign for most interacting pixel. Naively, we would expect supporting evidence for most pixels. However, this

phenomenon can be explained with the simple structure of the MNIST dataset. In general, the MNIST classification task can be solved with a few pixels up to high accuracy. Hence, the interaction is dominated by the relative accuracy of these *independent* predictors. Since these individual predictors are very accurate, the aggregation process itself does not add confidence to the prediction. The additional accuracy can solely be contributed to the original single pixels predictors and hence, we observe a negative interaction score. Consequently, our interaction measure reveals that the model mostly relies on a naive strategy of averaging accurate single pixel predictions. We point out, that this phenomenon is particular pronounced for figure eight, for which the super-pixel relevances are relatively small.

4.4. Regression: real-world NHANES dataset

In this section, we revisit the NHANES dataset (Cox et al., 1997) discussed at length in (Lundberg et al., 2020). It is a mortality dataset with 14,407 individuals and 79 features. The task is to predict the (log relative) risk of mortality. The main point we want to convey by this analysis is, that *PredDiff* provides similar quantitative insights into large real-world datasets compared to existing model-specific attribution frameworks. We train a *Random Forest* and compute relevances for the full set of individual features via Equation (3). We use the Mahalanobis imputer (Aas et al., 2019), which yielded more accurate imputations (when comparing the average imputation per sample with the ground

truth value) as the train set imputer, see Appendix H for different imputers and models.

The results on feature relevances are shown in the top panel of Figure 4. We infer global feature importances by computing the mean of the absolute relevance score for each feature across the whole test set. The three most important attributes agree with previous investigations in the literature (Lundberg et al., 2020), although the ordering of the features sex and systolic blood pressure is interchanged. Also the single feature relevances for the two most important continuous features age and systolic blood pressure are in qualitative agreement with earlier investigations.

The imputer choice can affect the relevances, although the global feature importance ranking, as well as the individual feature relevance plots, remain in qualitative agreement, see Appendix H. A detailed analysis on the impact of imputation quality on the accuracy of relevances is difficult to make for real-world datasets, where no ground truth is available, and therefore beyond the scope of this manuscript. Interestingly, also the model architecture has a pronounced effect even on the single feature relevances. When using a *gradient boosted decision tree* as considered in (Lundberg et al., 2020), there are even differences in terms of the global feature importance ranking. For example, systolic blood pressure, which was ranked second for the *Random Forest*, does not occur within the five most important features, see Appendix H. Instead, the white blood cell count is ranked third after age and sex according to global feature importance. Different feature importances for different algorithms are not surprising per se, but the tension between the *PredDiff* and the *TreeInterpreter* results is an interesting observation. This section is intended as a proof-of-principle demonstration. Detailed studies on model dependencies are therefore deferred to future work.

Turning to interaction relevances in the bottom panel of Figure 4, similar as for feature relevances, we assess the global interaction relevance from the mean absolute interaction relevances across the whole test set. Here, we consider all pairs of interactions between the five most important features identified in the first step. Systolic blood pressure and age, as well as age and sex, show pronounced interaction effects and the corresponding interaction relevances on a per-sample basis are again in qualitative agreement with literature results (Lundberg et al., 2020).

5. Conclusion

In this work, we revisited *PredDiff* as a model-agnostic attribution framework and introduced a concise notation to elaborate its main properties. Our main contribution is the introduction of a novel interaction measure. Lastly, we summarize the main advantages of *PredDiff*:

- **Conceptual simplicity:** For *well-calibrated* classifiers, *PredDiff* is deeply grounded in probability theory, see Equation (1). Additionally, interaction effect provide a novel argument in favor of *logarithmic differences*, as relevance measure. Overall, *PredDiff* is free of any conceptual ambiguities.
- **No reference points:** *PredDiff* does not rely on any reference points that are supposed to convey a complete absence of signal, which are, however, often ambiguously defined in practice.
- **Transparent imputation/Off-manifold:** Imputing samples is a necessary component for all perturbation-based approaches. *PredDiff* offers complete transparency through an *exchangable imputer*. In addition, a conditional sampler alleviates problems connected to classifier evaluation far from the data manifold.
- **Arbitrary feature sets:** *PredDiff* can adaptively evaluate relevances for *arbitrary sets of features*. These relevances naturally include *all interaction effects* (i.e. are inherently non-additive).
- **Error estimates:** *PredDiff* provides an *uncertainty estimate for relevances* on a per-sample basis.

Going beyond feature relevances as such, we would like to highlight:

- **Quantifying interaction effects:** *PredDiff* provides an explicit measure for *interaction relevances* between two disjoint feature sets, see Equation (6).
- **Linear Scaling:** Finally, and crucially for practical applications, both *PredDiff* relevances and interactions enjoy a *linear scaling with the number of features* under consideration. The scaling coefficient can readily be adjusted by varying the number of imputations, see Figure 2. Additionally, in practical applications often semantically meaningful feature combinations, rather than individual single features themselves, are the true objects of interests, see e.g. (Wei et al., 2018).

Following the MNIST example, many previous studies could directly leverage our results. We expect to see insights, that go far beyond conventional feature attributions alone, through a systematic investigation of interaction effects in more realistic use-cases and datasets.

Acknowledgements

This work was funded by the German Ministry for Education and Research as BIFOLD - Berlin Institute for the Foundations of Learning and Data (ref. 01IS18025A and ref. 01IS18037A).

References

- Aas, K., Jullum, M., and Løland, A. Explaining individual predictions when features are dependent: More accurate approximations to shapley values. *arXiv preprint 1903.10464*, 2019.
- Agarwal, C. and Nguyen, A. Explaining image classifiers by removing input features using generative models. In *Proceedings of the Asian Conference on Computer Vision*, 2020.
- Anders, C., Pasliev, P., Dombrowski, A.-K., Müller, K.-R., and Kessel, P. Fairwashing explanations with off-manifold detergent. In *International Conference on Machine Learning*, pp. 314–323. PMLR, 2020.
- Apley, D. W. and Zhu, J. Visualizing the effects of predictor variables in black box supervised learning models. *Journal of the Royal Statistical Society: Series B (Statistical Methodology)*, 82(4):1059–1086, 2020.
- Bach, S., Binder, A., Montavon, G., Klauschen, F., Müller, K.-R., and Samek, W. On pixel-wise explanations for non-linear classifier decisions by layer-wise relevance propagation. *PLoS ONE*, 10(7):e0130140, 07 2015. doi: 10.1371/journal.pone.0130140.
- Casalicchio, G., Molnar, C., and Bischl, B. Visualizing the feature importance for black box models. In Berlingero, M., Bonchi, F., Gärtner, T., Hurley, N., and Ifrim, G. (eds.), *Machine Learning and Knowledge Discovery in Databases*, pp. 655–670, Cham, 2019. Springer International Publishing.
- Covert, I., Lundberg, S., and Lee, S.-I. Feature removal is a unifying principle for model explanation methods. *arXiv preprint 2011.03623*, 2020.
- Cox, C., Mussolino, M., Rothwell, S., Lane, M., Golden, C., Madans, J., and Feldman, J. Plan and operation of the nhanes i epidemiologic followup study, 1992. *Vital and Health statistics. Ser. 1, Programs and Collection Procedures*, (35):1–231, 1997.
- Datta, A., Sen, S., and Zick, Y. Algorithmic transparency via quantitative input influence: Theory and experiments with learning systems. In *2016 IEEE symposium on security and privacy (SP)*, pp. 598–617. IEEE, 2016.
- Deng, H., Zou, N., Du, M., Chen, W., Feng, G., and Hu, X. A unified taylor framework for revisiting attribution methods. *arXiv preprint 2008.09695*, 2020.
- Fujimoto, K., Kojadinovic, I., and Marichal, J.-L. Axiomatic characterizations of probabilistic and cardinal-probabilistic interaction indices. *Games and Economic Behavior*, 55(1):72 – 99, 2006. ISSN 0899-8256. doi: 10.1016/j.geb.2005.03.002.
- Gosiewska, A. and Biecek, P. Do not trust additive explanations. *arXiv preprint 1903.11420*, 2020.
- Gu, J. and Tresp, V. Contextual prediction difference analysis for explaining individual image classifications. *arXiv preprint 1910.09086*, 2020.
- Guo, C., Pleiss, G., Sun, Y., and Weinberger, K. Q. On calibration of modern neural networks. In *International Conference on Machine Learning*, pp. 1321–1330. PMLR, 2017.
- Jakulin, A. and Bratko, I. Quantifying and visualizing attribute interactions. *arXiv preprint cs/0308002*, 2003.
- Janizek, J. D., Sturmfels, P., and Lee, S.-I. Explaining explanations: Axiomatic feature interactions for deep networks. *arXiv preprint 2002.04138*, 2020.
- Janzing, D., Minorics, L., and Bloebaum, P. Feature relevance quantification in explainable ai: A causal problem. In Chiappa, S. and Calandra, R. (eds.), *Proceedings of the Twenty Third International Conference on Artificial Intelligence and Statistics*, volume 108 of *Proceedings of Machine Learning Research*, pp. 2907–2916, Online, 26–28 Aug 2020. PMLR.
- Jin, X., Wei, Z., Du, J., Xue, X., and Ren, X. Towards hierarchical importance attribution: Explaining compositional semantics for neural sequence models. In *International Conference on Learning Representations*, 2020.
- Lemaire, V., Feraud, R., and Voisine, N. Contact personalization using a score understanding method. In *2008 IEEE International Joint Conference on Neural Networks (IEEE World Congress on Computational Intelligence)*. IEEE, June 2008. doi: 10.1109/ijcnn.2008.4633863.
- Lenis, D., Major, D., Wimmer, M., Berg, A., Sluiter, G., and Bühler, K. Domain aware medical image classifier interpretation by counterfactual impact analysis. In *International Conference on Medical Image Computing and Computer-Assisted Intervention*, pp. 315–325. Springer, 2020.
- Lundberg, S. M. and Lee, S.-I. A unified approach to interpreting model predictions. In *Advances in neural information processing systems*, pp. 4765–4774, 2017.
- Lundberg, S. M., Erion, G., Chen, H., DeGrave, A., Prutkin, J. M., Nair, B., Katz, R., Himmelfarb, J., Bansal, N., and Lee, S.-I. From local explanations to global understanding with explainable ai for trees. *Nature machine intelligence*, 2(1):2522–5839, 2020.
- Rezende, D. J., Mohamed, S., and Wierstra, D. Stochastic backpropagation and approximate inference in deep generative models. In Xing, E. P. and Jebara, T. (eds.),

- Proceedings of the 31st International Conference on Machine Learning*, volume 32 of *Proceedings of Machine Learning Research*, pp. 1278–1286, Beijing, China, 22–24 Jun 2014. PMLR.
- Ribeiro, M. T., Singh, S., and Guestrin, C. "why should i trust you?": Explaining the predictions of any classifier. *Proceedings of the 22nd ACM SIGKDD International Conference on Knowledge Discovery and Data Mining*, 2016.
- Robnik-Sikonja, M. and Kononenko, I. Explaining classifications for individual instances. *IEEE Transactions on Knowledge and Data Engineering*, 20(5):589–600, May 2008. doi: 10.1109/tkde.2007.190734.
- Schnake, T., Eberle, O., Lederer, J., Nakajima, S., Schütt, K. T., Müller, K.-R., and Montavon, G. Higher-order explanations of graph neural networks via relevant walks. *arXiv preprint 2006.03589*, 2020.
- Shapley, L. S. A value for n-person games,[in:] kuhn hw and tucker aw. *Contributions to the Theory of Games II*, pp. 307–317, 1953.
- Slack, D., Hilgard, S., Jia, E., Singh, S., and Lakkaraju, H. Fooling lime and shap: Adversarial attacks on post hoc explanation methods. In *Proceedings of the AAAI/ACM Conference on AI, Ethics, and Society*, AIES '20, pp. 180–186, New York, NY, USA, 2020. Association for Computing Machinery. ISBN 9781450371100. doi: 10.1145/3375627.3375830.
- Štrumbelj, E. and Kononenko, I. An efficient explanation of individual classifications using game theory. *J. Mach. Learn. Res.*, 11:1–18, March 2010. ISSN 1532-4435.
- Štrumbelj, E. and Kononenko, I. Explaining prediction models and individual predictions with feature contributions. *Knowledge and Information Systems*, 41(3):647–665, August 2013. doi: 10.1007/s10115-013-0679-x.
- Sundararajan, M. and Najmi, A. The many shapley values for model explanation. *arXiv preprint 1908.08474*, 2019.
- Sundararajan, M., Taly, A., and Yan, Q. Axiomatic attribution for deep networks. In *International Conference on Machine Learning (ICML)*, volume 70, pp. 3319–3328. JMLR, 2017.
- Sundararajan, M., Dhamdhere, K., and Agarwal, A. The shapley taylor interaction index. In III, H. D. and Singh, A. (eds.), *Proceedings of the 37th International Conference on Machine Learning*, volume 119 of *Proceedings of Machine Learning Research*, pp. 9259–9268. PMLR, 13–18 Jul 2020.
- Tian, S. and Cai, Y. Visualizing deep neural networks with interaction of super-pixels. In *Proceedings of the 2017 ACM on Conference on Information and Knowledge Management, CIKM '17*, pp. 2327–2330, New York, NY, USA, 2017. Association for Computing Machinery. ISBN 9781450349185. doi: 10.1145/3132847.3133108.
- Tsang, M., Rambhatla, S., and Liu, Y. How does this interaction affect me? interpretable attribution for feature interactions. In *Advances in neural information processing systems*, 2020.
- van Buuren, S. and Groothuis-Oudshoorn, K. mice: Multivariate imputation by chained equations inR. *Journal of Statistical Software*, 45(3), 2011. doi: 10.18637/jss.v045.i03. URL <https://doi.org/10.18637/jss.v045.i03>.
- Wei, Y., Chang, M.-C., Ying, Y., Lim, S. N., and Lyu, S. Explain black-box image classifications using superpixel-based interpretation. In *2018 24th International Conference on Pattern Recognition (ICPR)*. IEEE, August 2018. doi: 10.1109/icpr.2018.8546302.
- Zeiler, M. D. and Fergus, R. Visualizing and understanding convolutional networks. In Fleet, D., Pajdla, T., Schiele, B., and Tuytelaars, T. (eds.), *Computer Vision – ECCV 2014*, pp. 818–833, Cham, 2014. Springer International Publishing. ISBN 978-3-319-10590-1.
- Zhang, H., Xie, Y., Zheng, L., Zhang, D., and Zhang, Q. Interpreting multivariate shapley interactions in dnns. *arXiv preprint 2010.05045*, 2021.
- Zintgraf, L. M., Cohen, T. S., Adel, T., and Welling, M. Visualizing deep neural network decisions: Prediction difference analysis. In *International Conference on Learning Representations*, 2017.

A. Approximation using finite samples

We can approximate relevance, Equation (1), and the interaction relevance, Equation (6), by sampling from the respective conditional distributions, i.e.

$$\begin{aligned} m_{y|x_i}^f &= \int f(x_i, y)p(y|x_i)dy \\ &= \sum_{j:y_j \sim p(y|x_i)}^N f(x_i, y_j), \end{aligned} \tag{13}$$

for a potentially multidimensional y . As discussed in the main text, there are many perturbation-based attribution methods that can be understood as single sample ($N = 1$) approximations of *PredDiff*. In Figure 2 we show that a general trend is easily recovered with few samples but more samples are needed for high fidelity attributions.

Turning to the interaction relevance, where one additionally requires m -values of a slightly different structure, we find

$$\begin{aligned} m_{y|x_i}^{f|z=z_i} &= \int f(x_i, y, z_i)p(y|x_i)dy \\ &= \sum_{j:y_j, z_j \sim p(y, z|x_i)}^N f(x_i, y_j, z_i). \end{aligned} \tag{14}$$

This means we sample from $y_j, z_j \sim p(y, z|x_i)$ but discard z_j and replace the function argument by z_i instead. Again, a small sampling batch is sufficient to acquire reasonable accurate interaction attribution. In particular, interactions can be measured even if they are not yet visible in the single feature attributions.

B. Imputation algorithms for tabular data

In the accompanying code repository, we provide different popular imputers for tabular data.

Median Imputer: The *Median Imputer* replaces each column to be imputed by the corresponding median of the column in the training set. This imputer returns just a single imputation for each sample. The median imputer can be seen as analogue of classical occlusion methods (Zeiler & Fergus, 2014) in computer vision.

Train Set Imputer: The *Train Set Imputer* uses randomly sampled instances from the training set to impute respective values in the target columns. This was among the imputers proposed in the original *PredDiff* publication (Robnik-Sikonja & Kononenko, 2008).

Mahalanobis Imputer: The *Mahalanobis Imputer* (Aas et al., 2019) can be seen as a generalization of the *Train Set Imputer*. It also returns training set samples of the respective columns to be imputed but additionally provides a weighting factor. These weights are obtained from a kernel estimator based on the Mahalanobis distance.

Multivariate Gaussian Imputer: The *Multivariate Gaussian Imputer* samples from a multivariate, conditional Gaussian distribution that is conditioned on the values of the columns that are not to be imputed. In a *PredDiff* application in computer vision, a similar imputer was used in (Zintgraf et al., 2017).

Iterative Imputer: The *Iterative Imputer* uses multivariate imputation by chained equations (van Buuren & Groothuis-Oudshoorn, 2011), in a way comparable to the popular R-package *missForest*. The approach uses (Random Forest) predictors for every column conditioned on the remaining columns. The columns with missing values are initialized with the respective median values and are iteratively updated using the trained predictors until a fixed number of iterations is reached. To allow multiple imputations without retraining, for each predictor we sample from a Gaussian distribution with mean and variance determined by its constituent trees.

Variational Autoencoder with Pseudo-Gibbs Sampling: A trained variational autoencoder can be used for imputation by iteratively passing the sample through encoder and decoder. After each iteration values of columns not to be imputed

are restored. This procedure was shown to approximately sample from the desired conditional distribution (Rezende et al., 2014). In the MNIST example, we use fully connected encoders and decoders each with hidden units 500 and 256.

C. Properties of *PredDiff* relevances and interactions

C.1. Properties of *PredDiff* relevances:

We discuss basic properties of *PredDiff* relevances based on the five axioms investigated in (Sundararajan et al., 2017). In particular, these include the classic Shapley axioms (Shapley, 1953) *efficiency*, *linearity*, *symmetry* and *null player*. Properties of attribution methods are typically investigated in a regression setting and not investigated in a classification setting. The *PredDiff* formalism provides an explicit definition of the relevance in terms of calibrated class-wise output probabilities and therefore, allows to verify properties explicitly in the classification setting.

Completeness/Efficiency/Additivity/Local accuracy: The *completeness* axiom states that the summed relevances ϕ_i^f of all individual features i should yield the difference between the function value and a reference value, $f(x) = \phi_0^f + \sum_i \phi_i^f$. In the *PredDiff* framework relevances for individual features are not distinguished compared to those of arbitrary combinations of features. In particular, there is no reference value, which is either set explicitly as for Integrated Gradients (Sundararajan et al., 2017) or implicitly as for Shapley-values. In contrast, for every sample and feature combination there is a separate reference point for which the relevance vanishes.

Sensitivity/Dummy/Null Player/Missingness: Consider a function $f(x, y) = f(x)$ that does not depend on the features y . We find

$$m_{y|x_i}^f = \int f(x_i)p(y|x_i)dy = f(x_i) \quad (15)$$

and hence $\bar{m}_{y|x_i}^f = 0$ i.e. if f does not depend on y also the corresponding relevance is zero. This property holds both for classification and regression.

Linearity: For regression, one easily verifies that $\bar{m}_{y|x_i}^{af_1+bf_2} = a \cdot \bar{m}_{y|x_i}^{f_1} + b \cdot \bar{m}_{y|x_i}^{f_2}$. In a classification setting, linearity in the output probabilities themselves is not a natural assumption and the property is also not satisfied. Note that, even for factorizing functions, i.e. additive log probabilities, the relevances in general do not decompose into two separate contributions.

Symmetry: For a function $f(x, y, z)$ that is symmetric with respect to exchanging y and z , one easily verifies that also the relevances coincide i.e. $\bar{m}_{y|x_i,z_i}^f = \bar{m}_{z|x_i,y_i}^f$ if evaluated at $y_i = z_i$ provided that also the data distribution $p(x, y, z)$ shares the same symmetry with respect to exchanging y and z . The additional requirement on the data distribution is unavoidable for approaches that explicitly depend on the data distribution, as also realized in (Sundararajan & Najmi, 2019; Janzing et al., 2020) in slightly different contexts. This property holds both for classification and regression.

Implementation Invariance: The relevance is trivially independent of the way the function f is implemented as *PredDiff* is model-agnostic and only depends on the model outputs.

C.2. Properties of *PredDiff* interaction relevances

In this subsection, we discuss basic properties of the *PredDiff* interaction relevance.

No Interaction: In a regression setting, if f decomposes into a sum of two terms, each one depending only on one of the feature sets in question (y, z in this context) i.e. Equation (4), the interaction relevance between variables y and z vanishes $\bar{m}_{y;z|x_i}^{\text{int},f} = 0$.

In a classification setting, we require a vanishing interaction relevance in the case of generalized *informative conditional interactions* as specified in Equation (16) under the additional requirement on the data distribution that y and z are conditionally independent given x_i i.e. $p(y, z|x_i) = p(y|x_i) \cdot p(z|x_i)$. In this case, one can show $\bar{m}_{y;z|x_i}^{\text{int},f_c} = 0$, see Appendix D for a detailed derivation.

Null Player: If f does not depend on z , by the null player property for *PredDiff* relevances, we find $\bar{m}_{z|x_i}^{f|y=y_i} = 0$ and additionally $m_{yz|x_i}^f = m_{y|x_i}^{f|z=z_i}$. Hence, we find also $\bar{m}_{y;z|x_i}^{\text{int},f} = 0$. This property holds both for classification and regression.

Linearity: In a regression setting, one easily verifies that $\bar{m}_{y;z|x_i}^{\text{int},af_1+bf_2} = a \cdot \bar{m}_{y;z|x_i}^{\text{int},f_1} + b \cdot \bar{m}_{y;z|x_i}^{\text{int},f_2}$. As in the case of the *linearity* property for *PredDiff* relevances, linearity is not a sensible assumption in the classification and also not satisfied in the *PredDiff* formalism.

Symmetry: By construction, the interaction relevance is symmetric with respect to its arguments, i.e. $\bar{m}_{y;z|x_i}^{\text{int},f} = \bar{m}_{z;y|x_i}^{\text{int},f}$. This property holds both for classification and regression.

D. Interaction relevance for classification

We consider (non-overlapping) feature sets x, y, z that cover the set of all features and denote the label by c . In the following, we look at a generalization of *informative conditional interactions* (Jakulin & Bratko, 2003), i.e. interactions that satisfy $p(y, z|c) = p(y|c)p(z|c)$. Here, we consider a slight generalization, where y and z are assumed to be conditionally independent given c and x , $p(y, z|c, x) = p(y|c, x)p(z|c, x)$ or equivalently

$$p(y, z, x|c) = p(x, y|c)p(x, z|c). \quad (16)$$

Using Bayes' rule, we obtain for the class probability given the features

$$p(c|x, y, z) = p(c) \frac{p(x, y, |c)p(x, z|c)}{p(x, y, z)}. \quad (17)$$

Using this expression, one straightforwardly evaluates relevances

$$m_{y|xz}^{f_c} = p(c|x, z)p(x|c), \quad (18)$$

$$m_{z|xy}^{f_c} = p(c|x, y)p(x|c), \quad (19)$$

$$m_{yz|x}^{f_c} = \frac{p(c)}{p(x)} p(x|c)p(x|c). \quad (20)$$

From these expressions one derives centered (interaction) relevances

$$\bar{m}_{y|xz}^{f_c} = \log \left(\frac{p(x, y|z)p(x, z)}{p(x|c)p(x, y, z)} \right), \quad (21)$$

$$\bar{m}_{z|xy}^{f_c} = \log \left(\frac{p(x, z|y)p(x, z)}{p(x|c)p(x, y, z)} \right), \quad (22)$$

$$\bar{m}_{yz|x}^{f_c} = \log \left(\frac{p(x, y|c)p(x, z|c)p(x)}{p(x|c)p(x|c)p(x, y, z)} \right), \quad (23)$$

$$\begin{aligned} \bar{m}_{y;z|x}^{\text{int},f_c} &= \bar{m}_{y|xz}^{f_c} + \bar{m}_{z|xy}^{f_c} - \bar{m}_{yz|x}^{f_c} \\ &= \log \left(\frac{p(z|x)p(y|x)}{p(y, z|x)} \right), \end{aligned} \quad (24)$$

where the latter expression, which vanishes under the assumption that y and z are conditionally independent given x .

E. XOR classification example

To illustrate our interaction measure within a classification setting we use the xor-example defined by ($\epsilon > 0$)

$$p(c = 1|x, y) = \begin{cases} 1 - \epsilon & \text{if } x \neq y \\ \epsilon & \text{else} \end{cases} \quad (25)$$

and a uniform data distribution $p(x, y) = \frac{1}{4}$. Expressions for the alternative class $c = 0$ are mirror identical and therefore omitted. Starting from here we calculate the m -values

$$m_{x|y}^c = m_{y|x}^c = m_{x,y}^c = \frac{1}{2} \quad (26)$$

and deduce the interaction relevance

$$\bar{m}_{x;y}^{\text{int},c=1} = \begin{cases} \log(2(1-\epsilon)) & \text{if } x \not\leq y \\ \log(2\epsilon) & \text{else} \end{cases} . \quad (27)$$

This result aligns with our intuition and returns a positive (negative) interaction if $x \not\leq y$ is (not) satisfied for $\epsilon < \frac{1}{2}$.

F. Additional plots: synthetic dataset

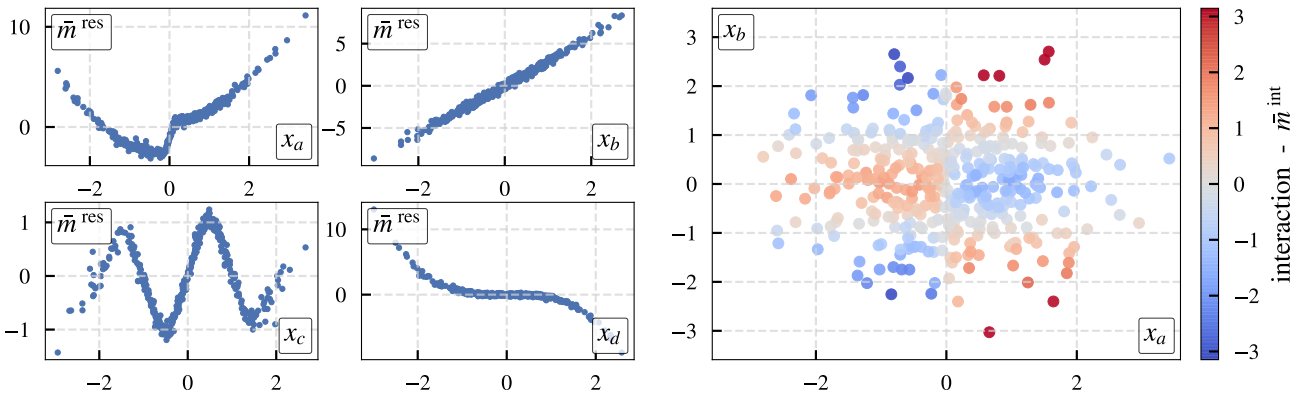


Figure 5. Fully-Connected Network analyzed with *PredDiff* for synthetic regression task. LEFT: $\bar{m}^{\text{res},f}$ according to Equation (7). RIGHT: color-encoded $\bar{m}^{\text{int},f}$ interaction relevance. Based on $N = 200$ imputations.

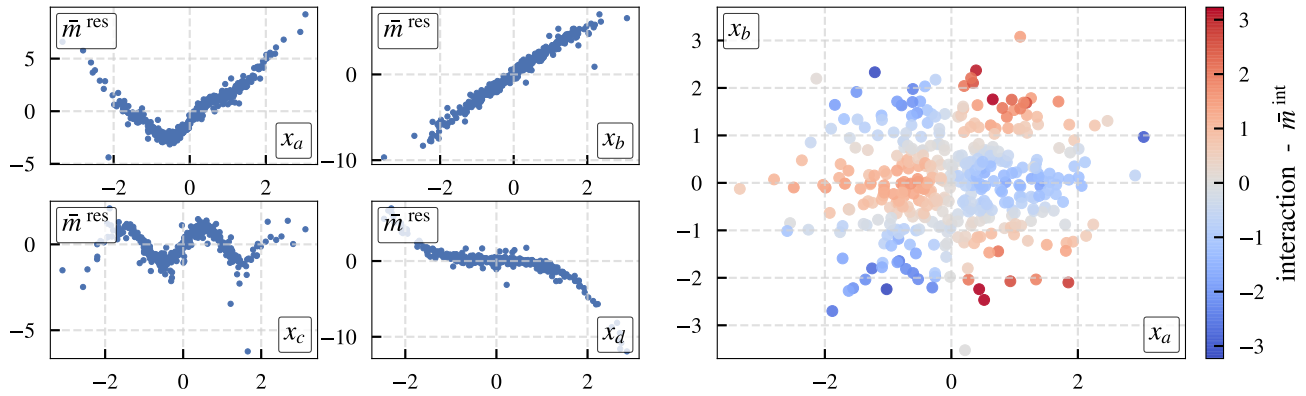


Figure 6. Gaussian Process analyzed with *PredDiff* for synthetic regression task. LEFT: $\bar{m}^{\text{res},f}$ according to Equation (7). RIGHT: color-encoded $\bar{m}^{\text{int},f}$ interaction relevance. Based on $N = 200$ imputations.

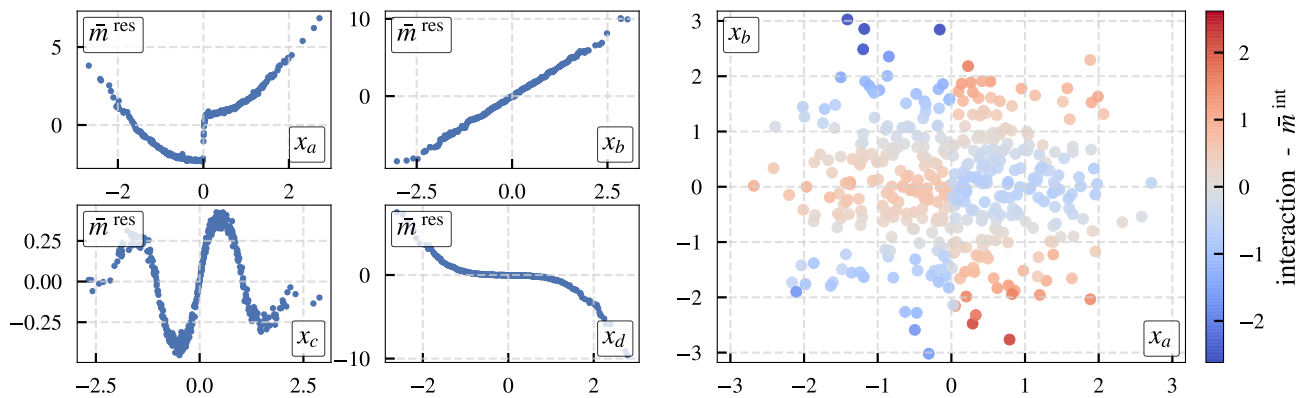


Figure 7. Model-aware SHAP TreeExplainer (Lundberg et al., 2020) applied on synthetic regression task. LEFT: residual contributions. RIGHT: interaction contribution for x_a, x_b .

G. Additional plots: MNIST

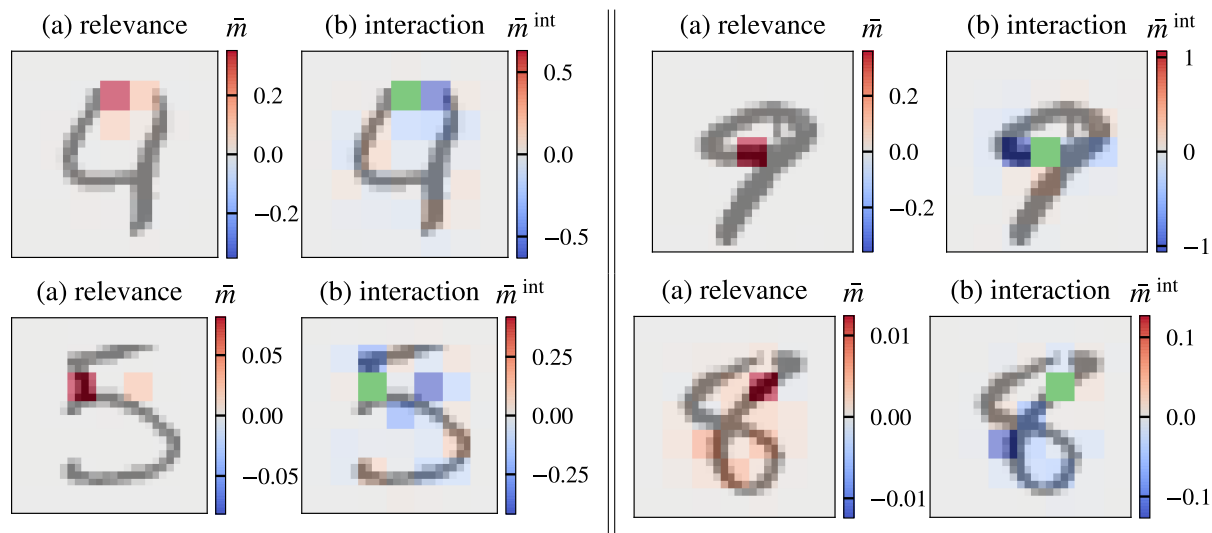


Figure 8. *PredDiff* for MNIST digits calculated on squared pixel batches ($\text{filter_size} = 4$) using a variational autoencoder with pseudo-Gibbs sampling (Rezende et al., 2014) as imputer. The improved and less diverse imputations, compared to the training set imputer, result in more sparse and focused attributions. (a) relevance. (b) interaction with respect to the marked (green) reference super-pixel. We always selected the super-pixel with highest relevance.

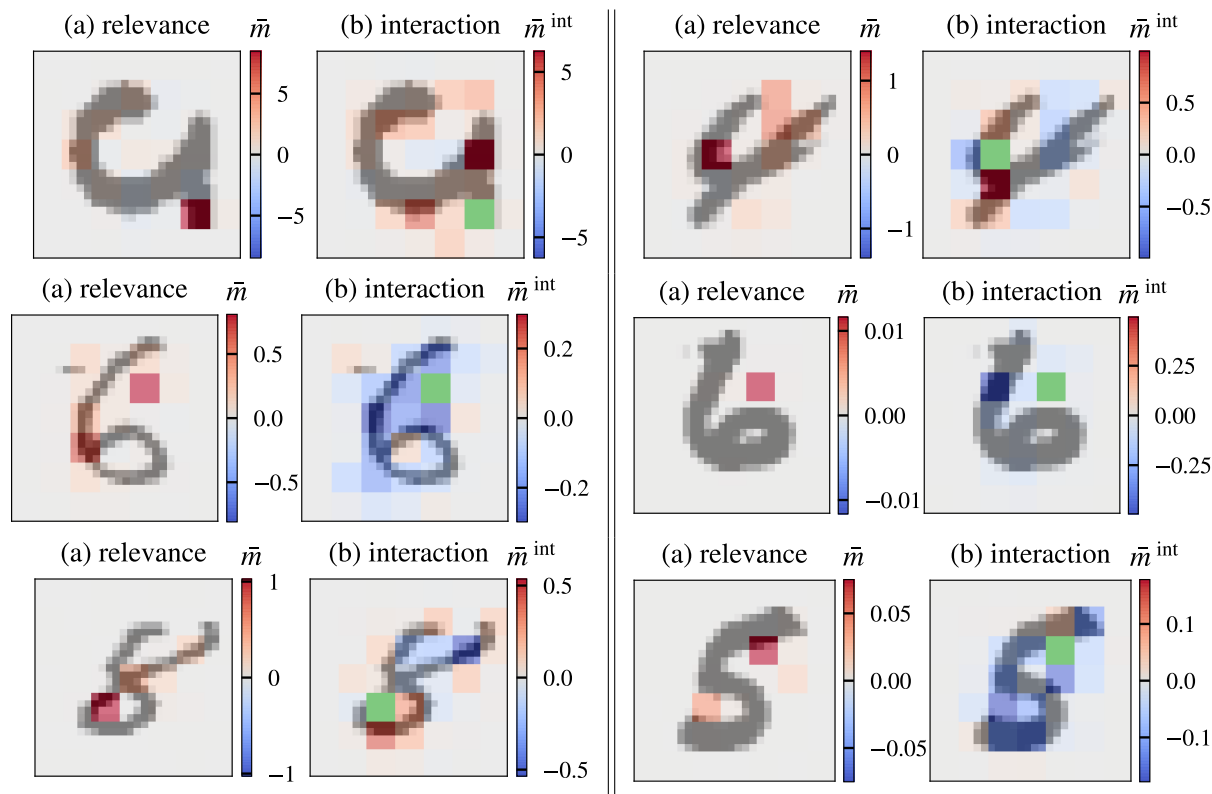


Figure 9. *PredDiff* for randomly selected MNIST digits calculated on squared pixel batches ($\text{filter_size} = 4$) using a train set imputer. (a) relevance. (b) interaction with respect to the marked (green) reference super-pixel. We always selected the super-pixel with highest relevance.

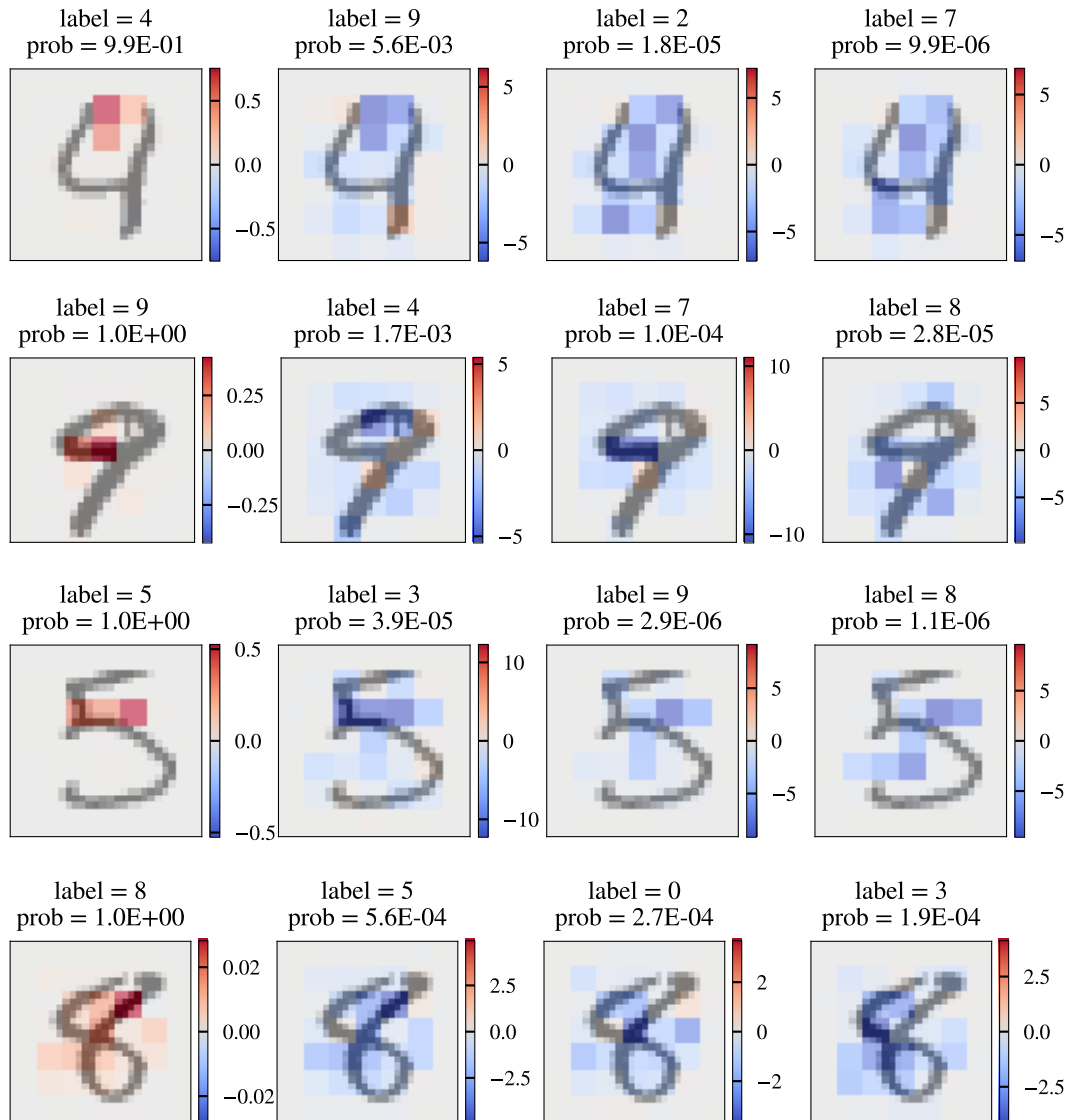


Figure 10. Investigating *PredDiff* relevances for classes with four highest prediction scores. Roughly speaking, this highlights which parts need to be altered to change the prediction, e.g. consider figure nine, here the upper loop should be opened to turn it into a four or seven.

H. Additional plots: NHANES

H.1. Random Forest

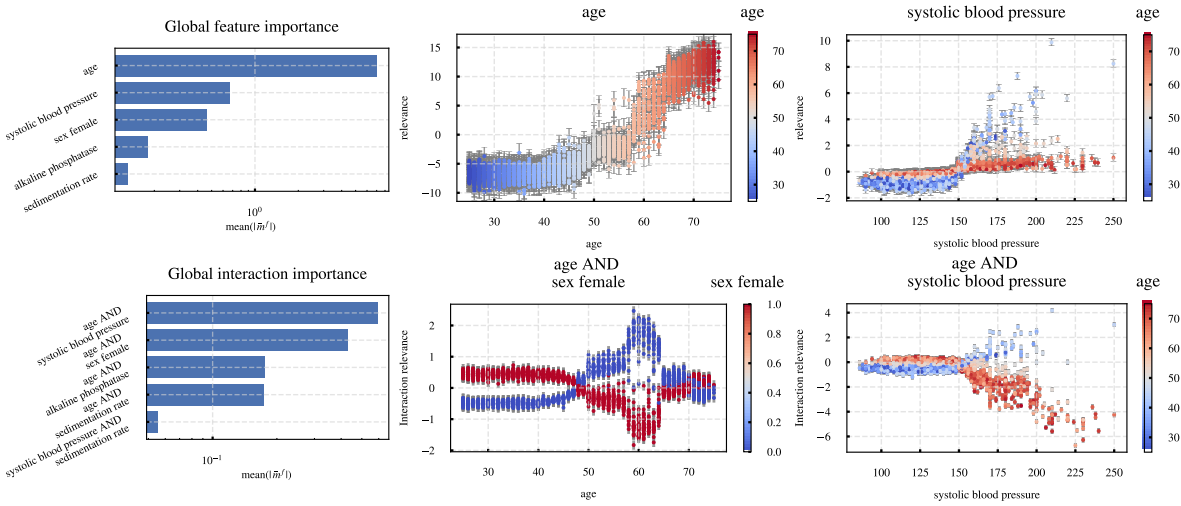


Figure 11. *PredDiff* (interaction) relevances for a *Random Forest* trained on the NHANES dataset using a *train set imputer*. TOP LEFT: Ranking of the five most important features TOP CENTER: Relevance for the most important feature age TOP RIGHT: Relevance for the second most important feature systolic blood pressure. BOTTOM LEFT: Ranking of the five most important feature interactions BOTTOM CENTER: Interaction relevance between age and sex BOTTOM RIGHT: Interaction relevance between systolic blood pressure and age.

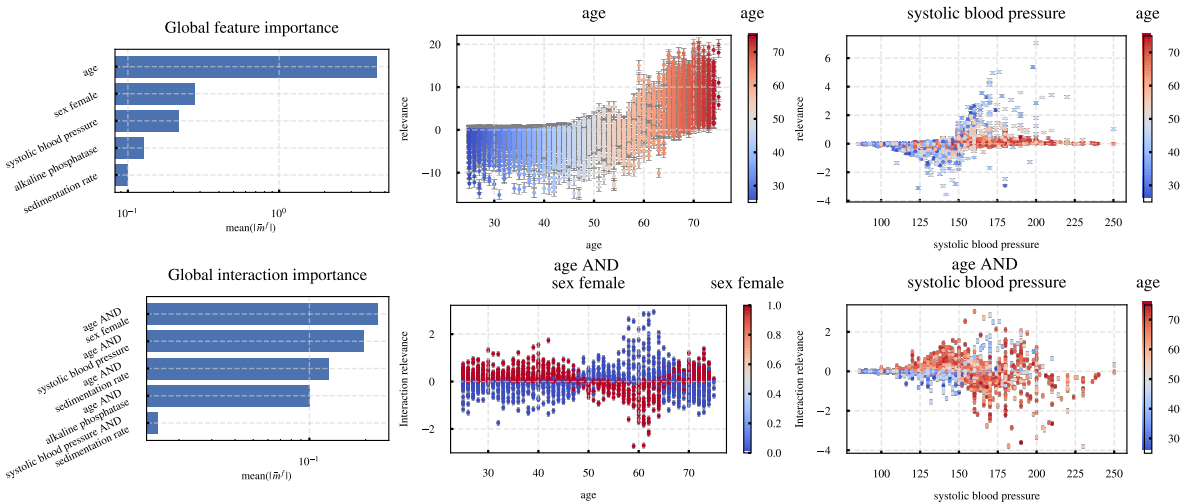


Figure 12. *PredDiff* (interaction) relevances for a *Random Forest* trained on the NHANES dataset using an *iterative imputer*. TOP LEFT: Ranking of the five most important features TOP CENTER: Relevance for the most important feature age TOP RIGHT: Relevance for the second most important feature systolic blood pressure. BOTTOM LEFT: Ranking of the five most important feature interactions BOTTOM CENTER: Interaction relevance between age and sex BOTTOM RIGHT: Interaction relevance between systolic blood pressure and age.

H.2. Boosted Decision Tree

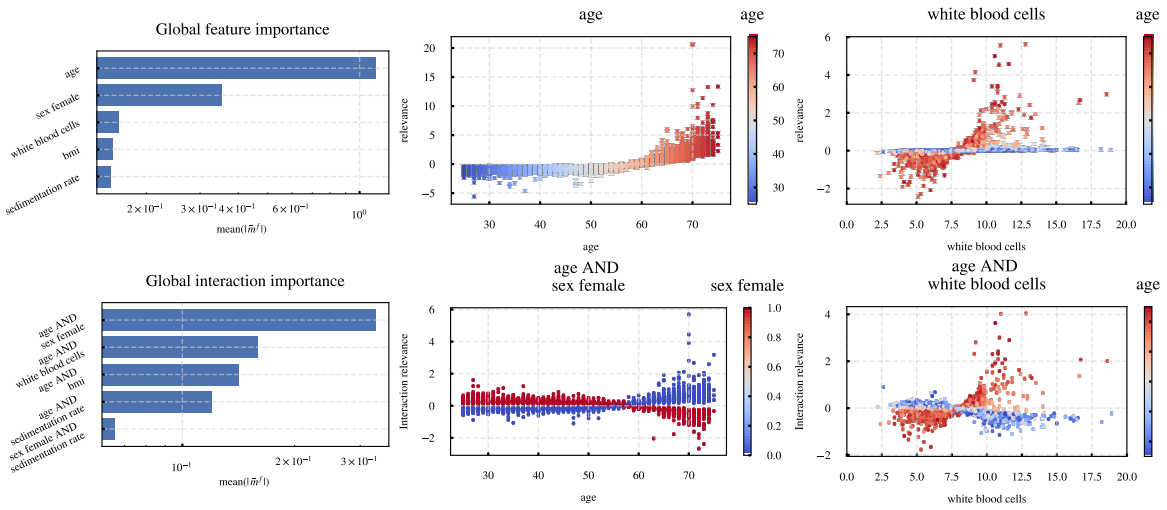


Figure 13. *PredDiff* (interaction) relevances for a *gradient-boosted decision tree* trained on the NHANES dataset using a *train set imputer*. TOP LEFT: Ranking of the five most important features TOP CENTER: Relevance for the most important feature age TOP RIGHT: Relevance for the second most important feature systolic blood pressure. BOTTOM LEFT: Ranking of the five most important feature interactions BOTTOM CENTER: Interaction relevance between age and sex BOTTOM RIGHT: Interaction relevance between white blood cell count and age.

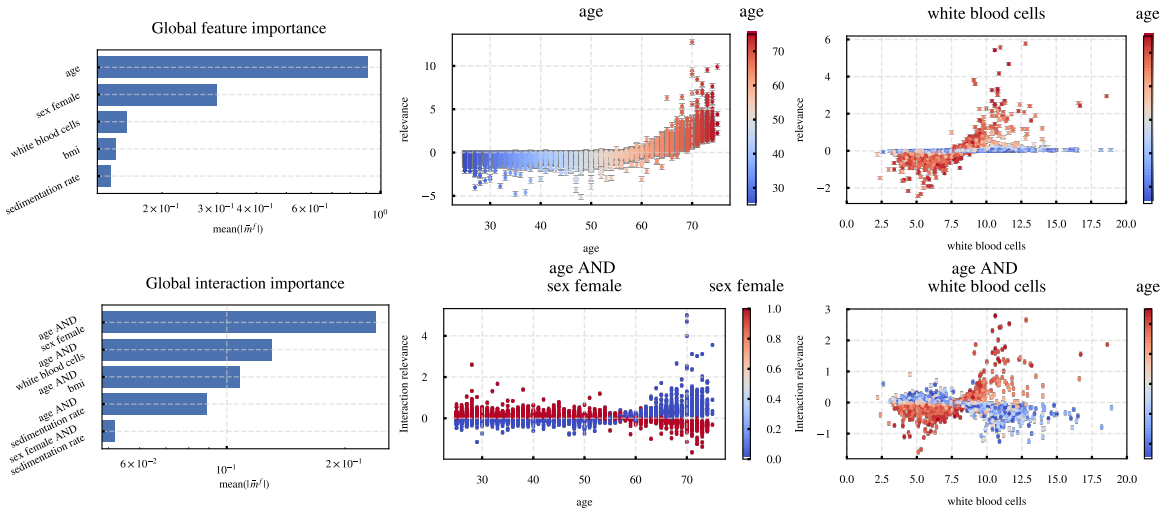


Figure 14. *PredDiff* (interaction) relevances for a *gradient-boosted decision tree* trained on the NHANES dataset using a *Mahalanobis imputer* (Aas et al., 2019). TOP LEFT: Ranking of the five most important features TOP CENTER: Relevance for the most important feature age TOP RIGHT: Relevance for the second most important feature systolic blood pressure. BOTTOM LEFT: Ranking of the five most important feature interactions BOTTOM CENTER: Interaction relevance between age and sex BOTTOM RIGHT: Interaction relevance between white blood cell count and age.

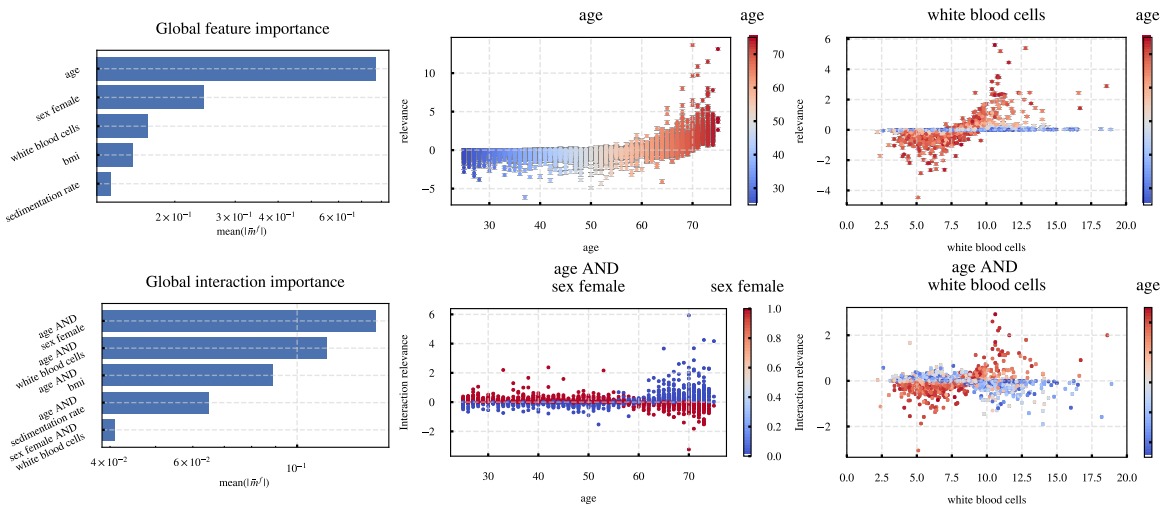


Figure 15. PredDiff (interaction) relevances for a *gradient-boosted decision tree* trained on the NHANES dataset using an *iterative imputer*. TOP LEFT: Ranking of the five most important features TOP CENTER: Relevance for the most important feature age TOP RIGHT: Relevance for the second most important feature systolic blood pressure. BOTTOM LEFT: Ranking of the five most important feature interactions BOTTOM CENTER: Interaction relevance between age and sex BOTTOM RIGHT: Interaction relevance between white blood cell count and age.